Electronic Supplementary Material (ESI) for Nanoscale.

Electronic Supplementary Information

"Revealing non-crystalline polymer superstructures within electrospun fibers through solvent-induced phase rearrangements"

Supplementary figures: Fig. S1-S8

Figure S1. Peak deconvolution of wide-angle X-ray scattering (WAXS) profiles.

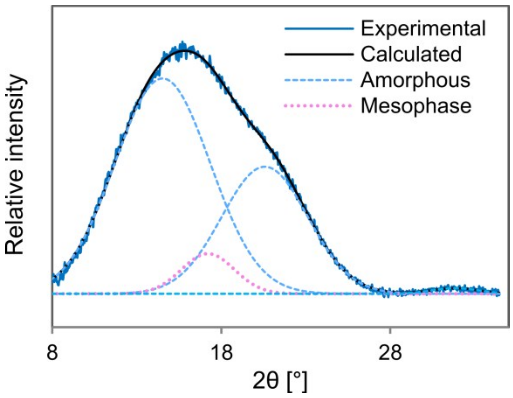

Fig. S1 Azimuthally integrated 1D-WAXS profile of as-spun fibers produced from DCM90: Peak deconvolution was carried out with Origin 2017 software (R^2=0.999). Amorphous phase is represented by dashed blue curves and mesophase by pink dotted curve.

Figure S2. 1D-WAXS and 1D-SAXS curves for DCM90 fibers treated in different acetone ratios.

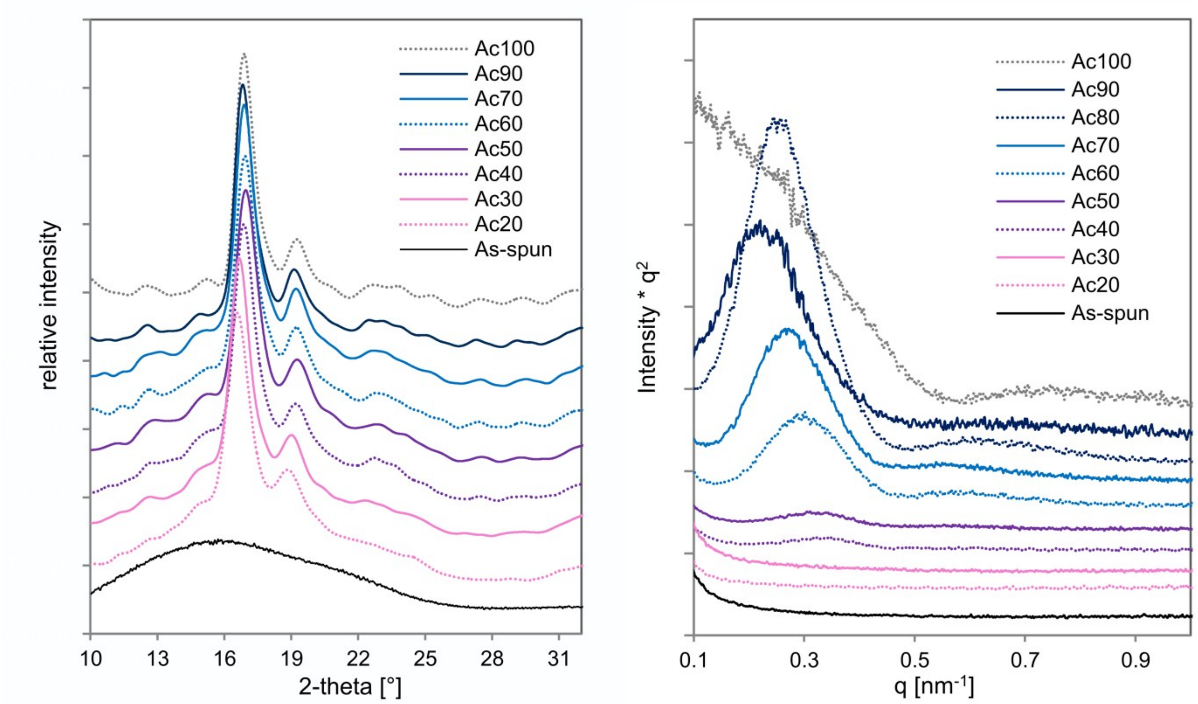

Fig. S2 (left) 1D-WAXS profiles of DCM90 fibers before and after SINC-treatment in different acetone ratios. (right) Corresponding Lorentz-corrected 1D-SAXS profiles obtained by 10°-azimuthal integration in the meridional section of the 2D-SAXS patterns. The samples were electrospun independently.

Figure S3. Orientation factor of the crystalline phase after SINC-treatment.

Azimuthal profiles were extracted from the 2D-WAXS patterns between 2θ = 15.5° – 18°, corresponding to the reflection peak of the (200)/(110) planes. The full width at half angle (FWHM) was then determined using Matlab software. The orientation factor was calculated according to the following equation.[1,2]

$$f_H = \frac{180° - FWHM}{FWHM}$$

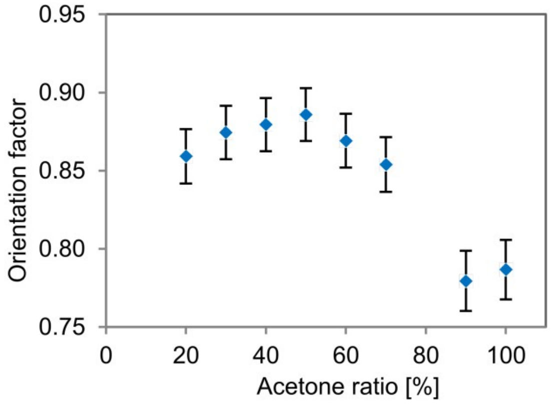

Fig. S3 Orientation factor of the (200)/(110) planes calculated from 2D-WAXS for DCM90 fibers treated in different acetone ratios. However, the moderate misalignment of the fibers is not taken into account.

Figure S4. Effect of the duration of treatment on the long period *L1*.

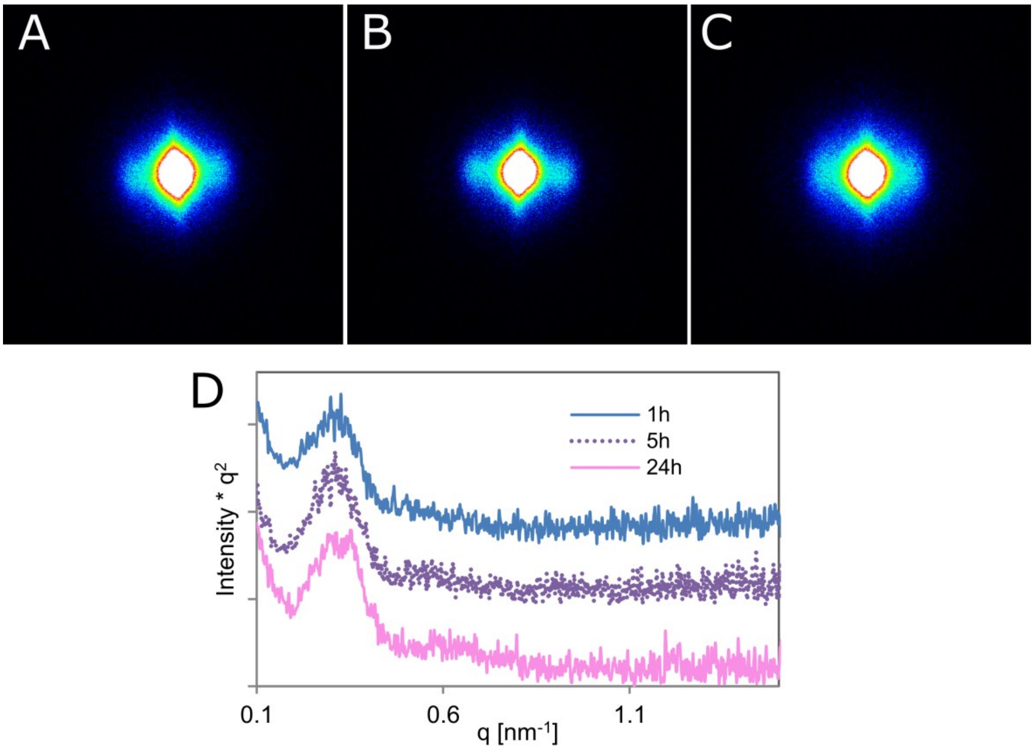

Fig. S4 2D-SAXS patterns of DCM90 aligned fibers treated in Ac50 for (a) 1h, (b) 5h and (c) 24h. (d) Corresponding Lorentz-corrected 1D-SAXS profiles. The calculated *L1*-values were 20.2 nm, 19.8 nm and 20.1 nm (±0.3 nm), respectively. The samples were electrospun independently.

Figure S5. Additional scanning electron microscopy images of e-spun fibers after SINC treatment.

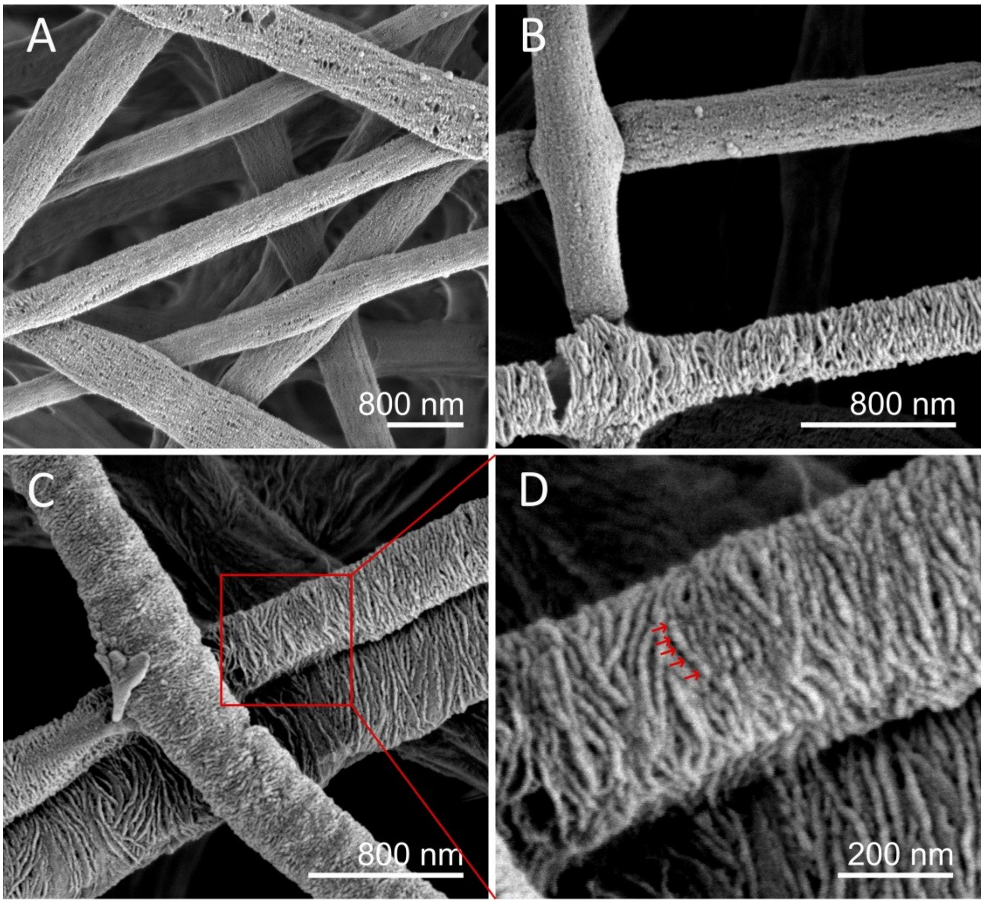

Fig. S5 (a-b) Fibers produced from DM90 and treated in Ac85. (a) DCM90 fibers with typical fibrillar structures at their surface. (b) The variety of fiber structure within a same sample is illustrated with a fiber incorporating large lamellar arrangements. (c) TFA100 fiber treated in Ac75 consisting of stacked lamellae of various sizes, with (d) showing the lamellae being composed of different granular blocks (red arrows).

Figure S6. Calculation of fibril width and lamellar spacing by SEM.

The width of nanofibrils (n = 18, among 6 fibers) was measured by ImageJ software by the use of SEM images of DCM90 fibers treated in Ac85. Only nanofibrils observable individually, i.e. with void on both sides, were considered (Fig. S6a). The width was measured between the crystallites disposed on the nanofibrils, since their width may have increased over the solvent treatment.

The lamellar spacing was calculated by measuring the length L_f along crystallites periodically disposed on a fibril (Fig. S6b), from the middle of the first crystallite to the middle of the last one. Then the spacing $L_{1,sem}$ was calculating by:

$$L_{1,sem} = \frac{L_f}{(N_c - 1)},$$

where N_c is the number of crystallites.

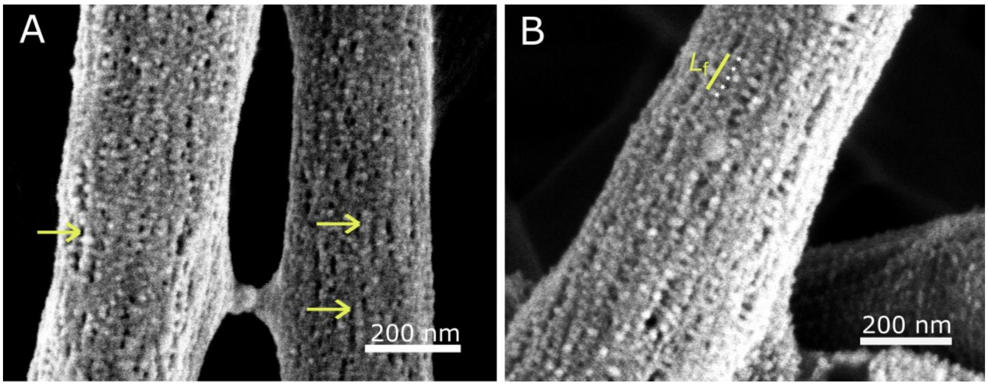

Fig. S6 SEM images of DCM90 fibers after AC85 treatment. The yellow arrows (a) show individual nanofibrils used for calculation of the width. The yellow bar (b) indicates the partial length of a fibril, the white stars correspond to crystallites disposed on the fibril.

Figure S7. Small-angle X-ray scattering (SAXS) profiles of as-spun fibers.

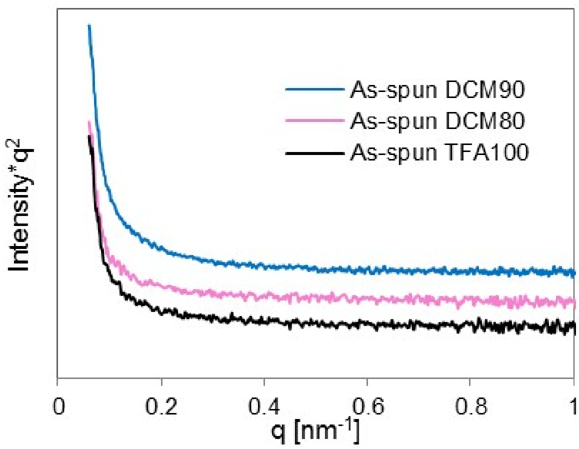

Fig. S7 1D-SAXS profiles of as-spun DCM90, DCM80 and TFA100 fibers. The profiles were obtained by the 10°-azimuthal integration of the 2D-patterns in the meridional direction after air background subtraction. No scattering peak is visible.

Figure S8. The two-electrode matrix collector.

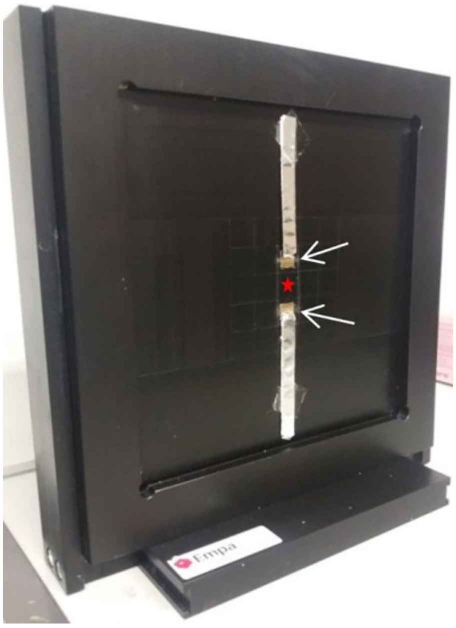

Fig. S8 In-house built collector consisting of two electrodes (white arrows) separated by 22 mm. Aligned fibers are collected between the electrodes (red star). An Aluminum stripe is attached to each electrode, modifying the shape of the electrical field and increasing the deposition rate of fibers between the electrodes.